

SAFT Modeling of the Solubility of Gases in Perfluoroalkanes

Ana M. A. Dias,[†] Josep C. Pàmies,[‡] João A. P. Coutinho,[†] Isabel M. Marrucho,[†] and Lourdes F. Vega^{*,§}

CICECO, Departamento de Química, Universidade de Aveiro, 3810-193 Aveiro, Portugal, Departament d'Enginyeria Química, ETSEQ, Universitat Rovira i Virgili, Avinguda dels Països Catalans, 26, 43007 Tarragona, Spain, and Institut de Ciència de Materials de Barcelona (ICMAB-CSIC), Campus de la UAB, 08193 Bellaterra, Barcelona, Spain

Received: July 29, 2003; In Final Form: November 20, 2003

A molecular model within a SAFT context for quantitatively predicting the solubility of xenon and oxygen in *n*-perfluoroalkanes is presented and discussed here. All species are treated as Lennard-Jones chains formed by tangentially bonded spheres with the same diameter and dispersive energy. Optimized meaningful values of both molecular parameters for the pure perfluoroalkanes are also used to accurately predict vapor–liquid and liquid–liquid equilibria of *n*-alkane + *n*-perfluoroalkane mixtures. Because of the high nonideality of the mixtures, the Lorentz–Berthelot cross-interaction parameters need to be adjusted using experimental data and ensuring coherent trends. An accurate description of the solubility of oxygen requires additional information to be included in the model. On the basis of ab initio arguments, we considered cross-association between oxygen and perfluoroalkane molecules, which allows solubilities to be described with a deviation below 5%, when compared to experimental data available in the literature and measured in our laboratory.

Introduction

Perfluoroalkanes are completely fluorinated alkanes with particular physicochemical properties due to the high intramolecular and low intermolecular forces that characterize them. Nowadays, they are being used in a widely variety of fields ranging from industrial to biomedical applications. In industry, they are being used as substitutes for chlorinated solvents due to the fact that they are nontoxic and do not deplete stratospheric ozone.¹ Furthermore, fluorinated solvents are immiscible with both hydrocarbons and water,² which facilitates their removal from the reaction medium by simple phase separation and filtration and also recycling of the solvent. Because of their high solubility in CO₂, fluorocarbons are currently employed as CO₂-philic compounds in many chemical and analytical applications where supercritical or liquid CO₂ is used as a “green” alternative to conventional organic solvents.³ For medical applications, perfluoroalkanes and other fluorinated liquids are used as oxygen carriers in artificial blood substitutes,⁴ because of the high solubility of oxygen in these compounds and their chemical and biological inertness. Liquid and gaseous perfluoroalkanes are also used as high-density intra-operative fluids for eye surgery.⁵ They show high solubilities of xenon as well, and for that reason, they are being used as intravenous delivery media for laser-polarized xenon for in vivo magnetic resonance applications.⁶

According to the exposed above, the study of the solubility of gases in liquids is still an actual issue due its importance in many industrial chemical processes, environmental studies, and also the medical field. From the fundamental scientific point of view, it also plays an important role in the understanding of the interactions among molecules. It is in this context that we

present this work. Empirical and semiempirical models, like traditional cubic equations of state (EOSs), have proved to have limited predictive capabilities, particularly outside the range where their parameters were fitted. On the other hand, molecular models based on statistical mechanics, as the statistical associating fluid theory (SAFT), use parameters with physical meaning and independent of the thermodynamic conditions. In addition, the use of these molecular based models allows one to explicitly consider intramolecular and/or intermolecular interactions among the chain molecules involved and to obtain additional information about the way molecules interact among themselves and with others when in solution.

There exist in the literature several works concerning the modeling of perfluorocarbon systems, including molecular simulations and EOSs. An effort has been devoted since some years ago toward the development of accurate force fields for the linear perfluoroalkanes.^{7,8} These force fields have been applied to predictions of phase equilibria and critical properties of pure perfluoroalkanes and the solubility of xenon in *n*-perfluorohexane.⁹ On the other hand, the SAFT-VR approach, in addition to the aforementioned systems, has also been used for the prediction of phase equilibria of alkane + perfluoroalkane mixtures.¹⁰ However, to our best knowledge, no modeling attempt of the solubility of oxygen in perfluoroalkanes within a SAFT context has been performed yet.

The goal of this work is to provide a reliable model based on a modified version of the SAFT equation, the so-called soft-SAFT^{7,12} EOS, for the prediction of the solubility of gases in perfluoroalkanes as well as the vapor liquid equilibria (VLE) and liquid–liquid equilibria (LLE) for *n*-alkane + *n*-perfluoroalkanes mixtures. This EOS is first applied to the study of mixtures of molecules with similar size, which is the case of the *n*-alkane + *n*-perfluoroalkanes mixtures. The study of the nonsimilar gas + perfluoroalkanes systems will provide information about the behavior of small inert molecules, such as

* To whom correspondence should be addressed. E-mail: lvega@icmab.es.
Phone: +34 93 580 18 53. Fax: +34 93 580 57 29.

[†] Universidade de Aveiro.

[‡] Universitat Rovira i Virgili.

[§] Institut de Ciència de Materials de Barcelona.

xenon, and small noninert molecules, such as oxygen, in solution with perfluoroalkanes. We do not apply SAFT to oxygen + alkane mixtures because of the unfeasibility of evaluating the model, since the existing experimental data are scarce and deviations among sources are significant.^{7–16}

In the next section, the soft-SAFT model, including a discussion on the physical meaning of parameters for the pure compounds, will be described. In the results and discussion section, SAFT predictions are compared to experimental data available in the literature for xenon + *n*-perfluoroalkane and *n*-alkane + *n*-perfluoroalkanes mixtures and measured in our laboratory in the case of oxygen + *n*-perfluoroalkanes. A discussion on the systematic improvement of the model is also outlined.

SAFT Modeling

The original SAFT EOS was proposed by Chapman et al.¹⁷ and Huang and Radosz,¹⁸ and it was derived from a first-order perturbation theory based on Wertheim's work.¹⁹ The success of the SAFT approach can be inferred from the large number of publications on the subject along the 14 past years. For details on the theory, its different versions and applications, the reader is referred to a pair of recent reviews,^{20,21} and references therein.

The SAFT EOS is generally formulated in terms of the residual molar Helmholtz energy, A^{res} , defined as the molar Helmholtz energy of the fluid relative to that of an ideal gas at the same temperature and density. A^{res} is written as the sum of three contributions:

$$A^{\text{res}} = A^{\text{total}} - A^{\text{ideal}} = A^{\text{ref}} + A^{\text{chain}} + A^{\text{assoc}} \quad (1)$$

A^{ref} accounts for the pairwise intermolecular interactions of the reference system, A^{chain} evaluates the free energy due to the formation of a chain from units of the reference system, and A^{assoc} takes into account the contribution due to site–site association. For molecules that do not associate, the association term is null.

The original SAFT is based on a hard-spheres reference fluid. In the soft-SAFT EOS, the reference term is a Lennard-Jones (LJ) monomer fluid, which accounts both for repulsive and attractive interactions. The reference term is calculated using the LJ EOS proposed by Johnson et al.¹⁹ When dealing with mixtures, we use the well-known van der Waals one-fluid mixing rules. For the determination of unlike parameters, the generalized Lorentz–Berthelot combining rules are employed:

$$\sigma_{ij} = \eta_{ij} \frac{\sigma_{ii} + \sigma_{jj}}{2} \quad (2)$$

$$\epsilon_{ij} = \xi_{ij} \sqrt{\epsilon_{ii} \epsilon_{jj}} \quad (3)$$

where η and ξ are the binary parameters for the species i and j .

Based on the polymerization limit of Wertheim's theory, A^{chain} is obtained as a function of the chain length m and the pair correlation function of the reference fluid. Hence, the radial distribution function of LJ monomers g_{LJ} is used in the soft-SAFT EOS. The dimensionless form of the chain contribution is

$$\tilde{A}^{\text{chain}} = \tilde{T} \sum_i x_i (1 - m_i) \ln[g_{\text{LJ}}(\tilde{\sigma}_{ii})] \quad (4)$$

where Avogadro's number, N_A , the Boltzmann constant, k_B , and

the temperature, $T = \tilde{T}\epsilon/k_B$, appear in the dimensionless molar free energy $\tilde{A}^{\text{chain}} = A^{\text{chain}}/N_A k_B T$ and x_i is the mole fraction of component i .

The association term, within the first-order Wertheim's perturbation theory for associating fluids, is expressed as the sum of the contributions of all associating sites of component i . The dimensionless expression is

$$\tilde{A}^{\text{assoc}} = \tilde{T} \sum_i x_i \left(\sum_{\alpha} \left[\ln X_i^{\alpha} - \frac{X_i^{\alpha}}{2} \right] + \frac{M_i}{2} \right) \quad (5)$$

M_i is the number of associating sites of component i , and X_i^{α} is the mole fraction of molecules of component i not bonded at site α , which accounts for the contributions of all of the associating sites in each species

$$X_i^{\alpha} = \frac{1}{1 + \tilde{\rho} \sum_j x_j \sum_{\beta} X_j^{\beta} \tilde{\Delta}^{\alpha\beta_j}} \quad (6)$$

where $\tilde{\rho} = \rho N_A \sigma^3$ is the nondimensional density and $\tilde{\Delta}^{\alpha\beta_j}$ is related to the strength of the association bond between site α in molecule i and site β in molecule j . For the square-well bonding potential and the geometry of the association sites (see reference²⁰ for details), the simplified expression is

$$\tilde{\Delta}^{\alpha\beta_j} = 4\pi \left(\exp \left[\frac{\epsilon^{\alpha\beta_j}}{\tilde{T}} \right] - 1 \right) \tilde{k}^{\alpha\beta_j} \tilde{I} \quad (7)$$

Parameter $\tilde{\epsilon}^{\alpha\beta_j}$ is the depth of the square-well site reduced by the LJ core energy, and $\tilde{k}^{\alpha\beta_j}$ is related to the volume available for bonding. \tilde{I} is an integral which, in the soft-SAFT approach, includes the radial distribution function of LJ monomers and it has been numerically evaluated for the square-well geometry.²³

In a simplified picture of a pure SAFT nonassociating fluid, molecules are seen as homonuclear chains composed of equal spherical segments bonded tangentially. Different fluids will have a different number of segments, m , segment diameter, σ , and segment interaction energy, ϵ . For molecules that may associate, the association energy parameter, ϵ^{ij} and the association volume parameter k^{ij} are also defined to characterize the interactions between the associating sites of species i and j . In this work, we consider all associating sites in a molecule to be identical, $\epsilon^{ij} = \epsilon^{\alpha\beta_j}$ and $k^{ij} = k^{\alpha\beta_j}$.

Values for the molecular parameters of pure compounds are usually adjusted by minimizing deviations from the theory with respect to VLE experimental data. Nevertheless, whenever possible, it is of worth to use physical information in order to minimize the number of parameters to be optimized. In this manner, we set the m parameter of xenon to unity because it is spherical. Furthermore, experimental studies indicate that C–C bond lengths for crystalline poly(tetrafluoroethylene) and polyethylene are equivalent;⁷ hence, we set the values of the m parameter for *n*-perfluoroalkanes equal to those optimized for the *n*-alkanes in a previous work.²⁴ The remaining molecular parameters of the nonassociating model for the pure compounds were calculated by fitting vapor pressures and saturated liquid densities to experimental data away from the critical region, and they are listed in Table 1. *n*-Perfluorooctane is the heaviest member of the series for which enough experimental data is available in the literature.

From the optimized parameters for the perfluoroalkanes, we provide a simple relationship of the molecular parameters with

TABLE 1: Optimized Molecular Parameters for the Pure Components

	<i>m</i>	σ (Å)	ϵ/k_B (K)
O ₂	1.168	3.198	111.5
Xe	1.000	3.953	226.6
CF ₄	1.000	4.217	190.1
<i>n</i> -C ₂ F ₆	1.392	4.342	204.5
<i>n</i> -C ₃ F ₈	1.776	4.399	214.7
<i>n</i> -C ₄ F ₁₀	2.134	4.433	223.0
<i>n</i> -C ₅ F ₁₂	2.497	4.449	230.2
<i>n</i> -C ₆ F ₁₄	2.832	4.479	236.6
<i>n</i> -C ₇ F ₁₆	3.169	4.512	242.7
<i>n</i> -C ₈ F ₁₈	3.522	4.521	245.1

the carbon number in eqs 8–10. Units of σ and ϵ/k_B are Å and K, respectively

$$m = 0.3580CN + 0.6794 \quad (8)$$

$$m\sigma^3 = 35.53CN + 42.27 \quad (9)$$

$$m\epsilon/k_B = 96.42CN + 92.25 \quad (10)$$

Parameters from these relationships deviate from the fitted parameters with an absolute averaged deviation (AAD) equal to 0.8%. Equations 8–10 allow the transferability of parameters within the perfluoroalkane series.

One of the advantages of molecular theories compared to macroscopic models is that the formers need fewer parameters which are meaningful. To provide additional evidence of this, optimized size and energy parameters are plotted in Figure 1 with respect the carbon number *CN* of the *n*-perfluoroalkane chain. Because the model is homonuclear and the effect of the extreme CF₃ groups weakens as the chain length increases, the LJ parameters should tend to an asymptotic value, as seen in Figure 1. Furthermore, molecular simulation united-atom models^{7,25} in which the LJ potential for the nonbonded interactions is used (without Coulombic interactions), employ optimized values for the size parameter in the range $\sigma_{CF_2} = \sigma_{CF_3} = 4.65 \pm 0.05$ Å. These simulations give quantitative predictions for equilibrium properties of chains from *n*-perfluoropentane to *n*-perfluorohexadecane. The corresponding value from our model (equivalent to a chain of infinite number of carbons), straightforwardly calculated from eqs 8–10, is 4.63 Å. The similarity among the parameters of different theories acts in favor of the physical meaning of them.

Results and Discussion

Once a molecular model in the SAFT framework is defined and appropriate values for the molecular parameters of pure compounds have been determined, we use the soft-SAFT EOS to predict the equilibrium properties of several mixtures of *n*-alkane + *n*-perfluoroalkane and the solubility of xenon and oxygen in *n*-perfluoroalkanes from C₆ to C₉. Then, the accuracy of SAFT predictions will show the suitability of the molecular model for these perfluorocarbon systems.

In Figure 2, parts a and b, vapor–liquid coexisting densities and vapor pressures, respectively, of pure oxygen and pure xenon are shown. Symbols are experimental data taken from NIST Chemistry Webbook,²⁵ whereas solid lines correspond to the soft-SAFT EOS. Subcritical equilibrium properties are accurately reproduced. Because of the classical formulation of the equation as it is used here, temperatures and pressures in the critical region are overpredicted. There exist ways to overcome this problem, either by fitting parameters to the critical

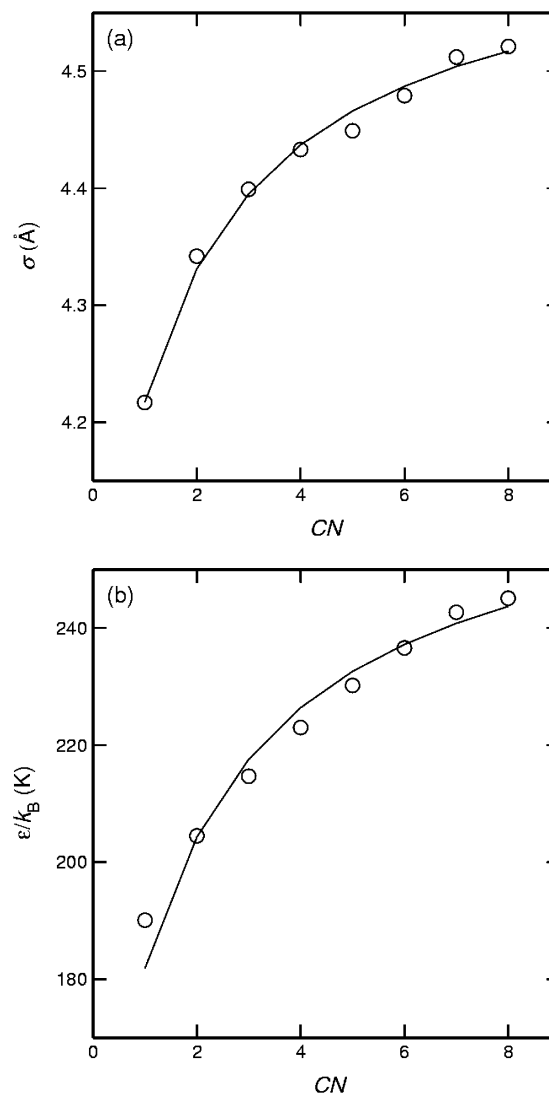


Figure 1. Molecular parameters for *n*-perfluoroalkanes: (a) segment diameter; (b) dispersive energy. Lines correspond to the values from the relationships of eqs 8–10.

point²⁷ or, in a more fundamental approach, including a crossover treatment.²⁸ Any of the methods will necessarily require of additional parameters or, at least, a new fitting to experimental data. Thus, because this work is focused on equilibrium properties far from the critical region, and also for consistency with previous works,^{24,27} we use parameters fitted to subcritical VLE data.

Figure 3, parts a and b, presents equilibrium liquid densities and vapor pressures, respectively, of pure *n*-perfluoroalkanes from *n*-perfluorohexane to *n*-perfluorooctane. Lines are soft-SAFT predictions using the parameters given in Table 1. Experimental saturated liquid densities and vapor pressures are correlated with an AAD less than 0.5% and 7%, respectively. In the case of *n*-perfluorononane, because only experimental density data are available,²⁹ we used the correlations of parameters for the *n*-perfluoroalkane series given by eqs 8–10. The agreement of the predicted density, with an AAD of 0.21%, is good, as for the rest of the perfluoroalkanes studied.

A more severe way to test the model and parameters for the perfluoroalkanes is to predict equilibrium curves of highly nonideal mixtures and compare them to experimental data. As a first case, we selected several *n*-alkane + *n*-perfluoroalkane mixtures of similar chain-length components and make use of

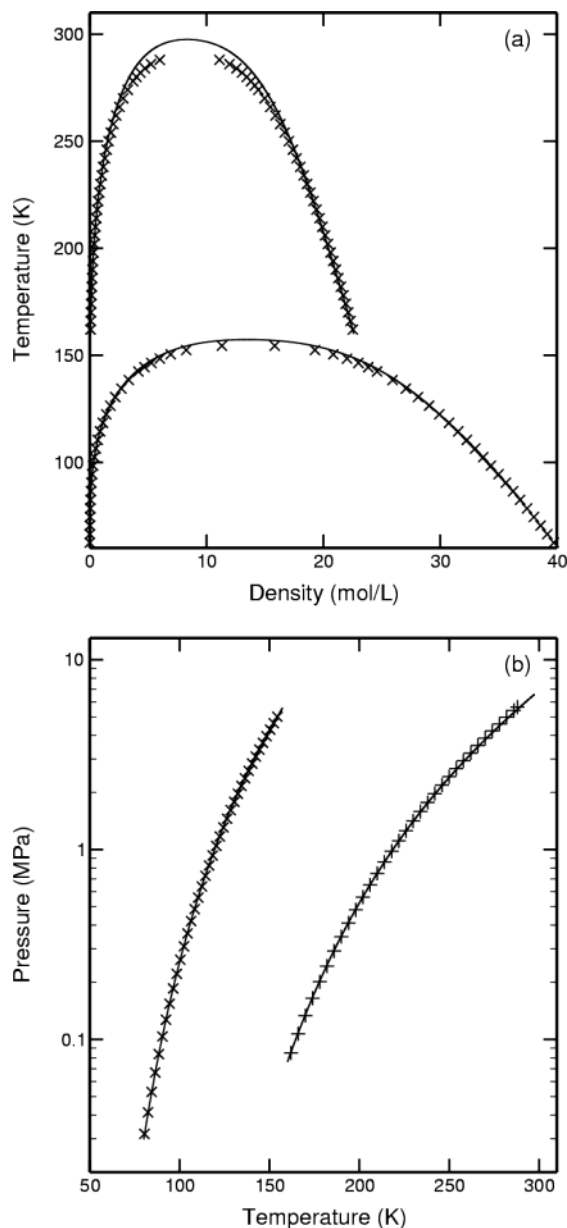


Figure 2. (a) Coexisting densities and (b) vapor pressures of pure oxygen (crosses) and xenon (pluses). Symbols are experimental data from the NIST chemistry Webbook,²⁵ and lines correspond to the soft-SAFT model with optimized parameters.

the fact that the molecular model and parameters for the normal alkanes have been broadly tested in previous works.^{24,32}

Equilibrium diagrams of binary mixtures of *n*-perfluorohexane + *n*-alkane from (C₅–C₈) and of *n*-hexane + *n*-perfluoroalkane from (C₅–C₈) are presented in Figures 4–7. These binary *n*-alkane + *n*-perfluoroalkane mixtures belong to the type II phase behavior in the classification of Scott and van Konynenburg³³ (characterized by a continuous vapor–liquid critical line and the presence of liquid–liquid phase separation) when the difference in chain length between the two components is not very large. Because of the nonideal interactions in these mixtures, the unlike energy parameter was treated as adjustable, and it was set at the optimum value $\xi = 0.9146$ for the correct prediction of the experimental azeotrope³⁴ of the *n*-hexane + *n*-perfluorohexane mixture at 298.15 K. Afterward, in a transferable manner, we used the same optimized value to predict the rest of the mixtures at different thermodynamic conditions. The unlike size parameter was not adjusted ($\eta =$

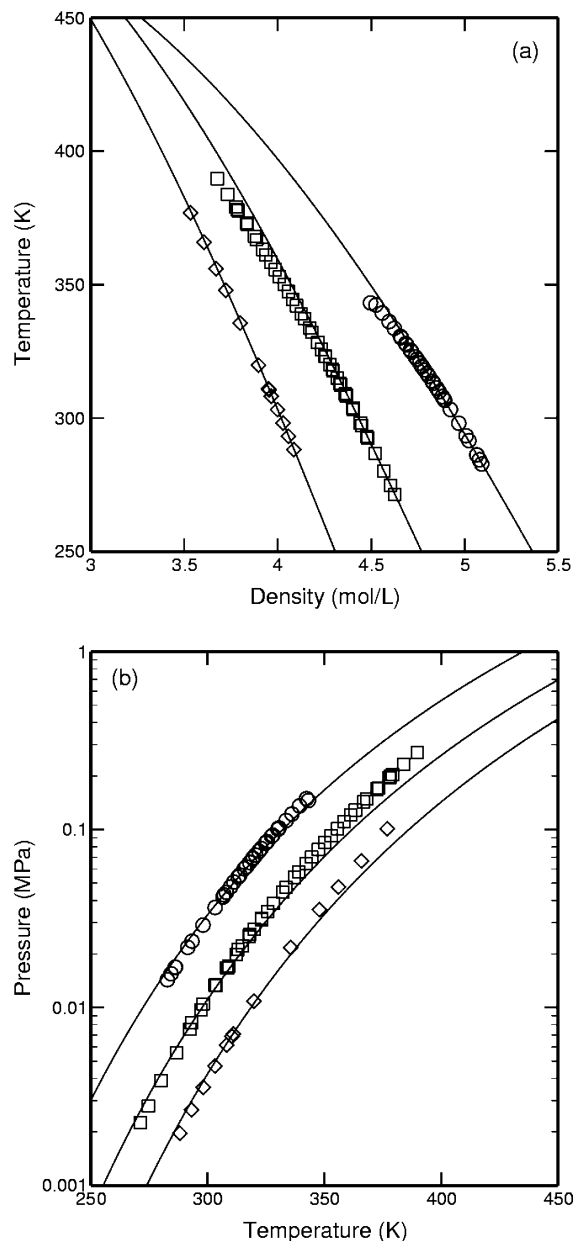


Figure 3. (a) Coexisting densities and (b) vapor pressures of *n*-perfluorohexane (circles), *n*-perfluoroheptane (squares), and *n*-perfluorooctane (diamonds). Symbols are experimental data (vapor pressures from ref 29 for C₆,³⁰ for C₇,³¹ for C₈, and densities from ref 38), and lines correspond to the soft-SAFT model with optimized parameters.

1), because we verified that the simple Lorentz combination rule provided satisfactory results.

Figures 4 and 5 present composition diagrams of *n*-hexane + *n*-perfluoroalkane and *n*-perfluorohexane + *n*-alkane mixtures, respectively, and Figure 6 depicts vapor pressures of two of the systems shown in Figure 5. Very good agreement is obtained between soft-SAFT predictions and experimental data³⁴ in all cases, considering that the average uncertainty of the experimental compositions is 4%. The AADs of the soft-SAFT predictions for compositions and pressures are less than 5% in all of the cases. At this point, it is worth mentioning that certain values of the binary parameters can originate s-shaped curves in the composition diagrams, wrongly predicting LLE. This is more likely to happen when one tries to reproduce vapor pressures with better accuracy than compositions. We could adjust the binary interaction parameters to completely avoid the

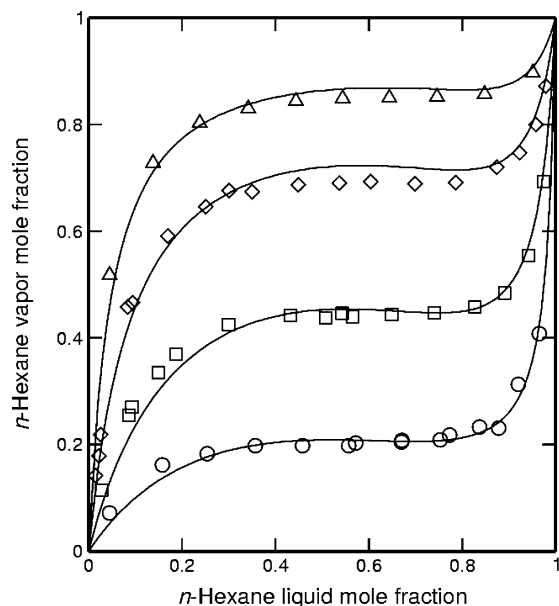


Figure 4. Vapor-phase mole fraction versus the liquid mole fraction for *n*-hexane + *n*-perfluoroalkane mixtures: *n* = 5 at 293.15 K (circles), *n* = 6 at 298.15 K (squares), *n* = 7 at 303.15 K (diamonds), and *n* = 8 at 313.15 K (triangles). Symbols represent experimental data,³⁴ and lines correspond to the predictions from the soft-SAFT EOS.

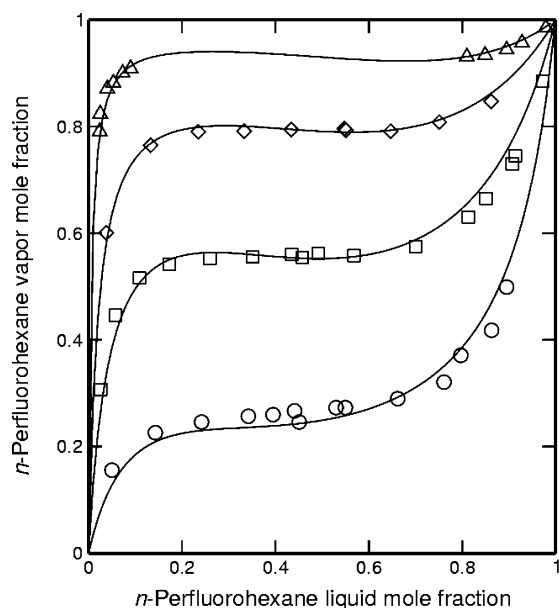


Figure 5. Vapor-phase mole fraction versus the liquid mole fraction for *n*-perfluorohexane + *n*-alkane mixtures: *n* = 5 at 293.65 K (circles), *n* = 6 at 298.15 K (squares), *n* = 7 at 317.65 K (diamonds), and *n* = 8 at 313.15 K (triangles). Symbols represent experimental data,³⁴ and lines correspond to the predictions from the soft-SAFT EOS.

appearance of s-shaped lines, but then deviations from experiments will largely increase. Therefore, because we want to retain this approximate model with the minimum parametrization, we should find a compromise. Consequently, although we tried to minimize the problem of s-shaped lines in Figures 4–6, we preferred to focus on the quantitative prediction of vapor–liquid equilibrium compositions. These systems have also been studied by McCabe et al.¹⁰ and Colina et al.³⁵ using the SAFT-VR approach. Because they focused on the critical region, using rescaled parameters to the critical points of the pure components, the predictions that they provide for subcritical properties are fairly less accurate.

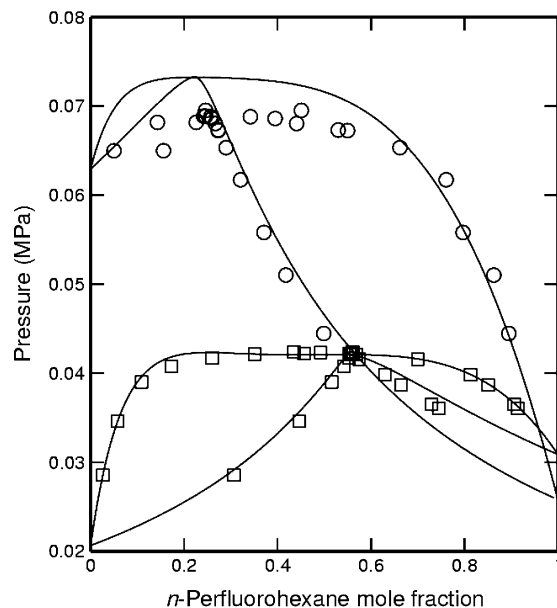


Figure 6. Vapor pressures of *n*-perfluorohexane + *n*-pentane and *n*-perfluorohexane + *n*-hexane. Thermodynamic conditions and symbols as in Figure 5.

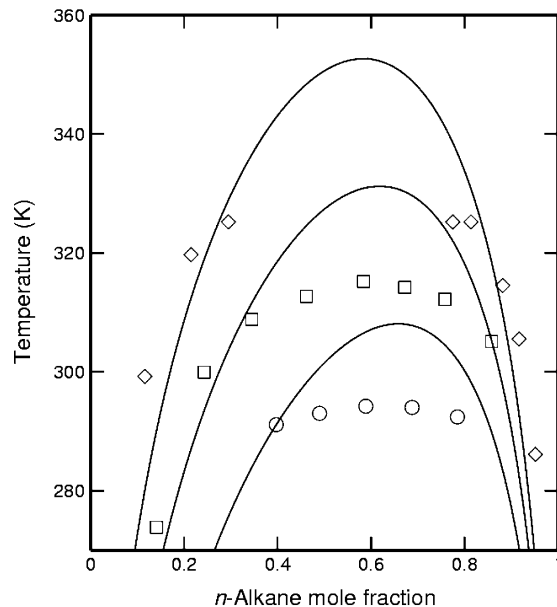


Figure 7. LLE of *n*-perfluoroalkane + *n*-alkane mixtures at 0.1 MPa: *n* = 6 (circles), *n* = 7 (squares), and *n* = 8 (diamonds). Symbols represent experimental data.³⁴ Solid lines correspond to the predictions from the soft-SAFT EOS.

We also performed calculations of LLE properties for the systems for which experimental data are available,³⁴ and they are presented in Figure 7. As a further verification of the transferability of parameters, we took the same values for the binary energy parameters used in the former VLE predictions, and hence, no fitting to LLE data was done. Because the equation as it is used here does not correctly model the critical region, we expected SAFT to overpredict the UCST. However, although most of the experimental points are located in the critical region, it is observed that the shape of the curve is correct and the quantitative prediction of the low-temperature region is acceptable.

As a summary up to this point, the soft-SAFT model presented here allows the phase behavior of *n*-alkane + *n*-perfluoroalkanes of similar chain length to be quantitatively

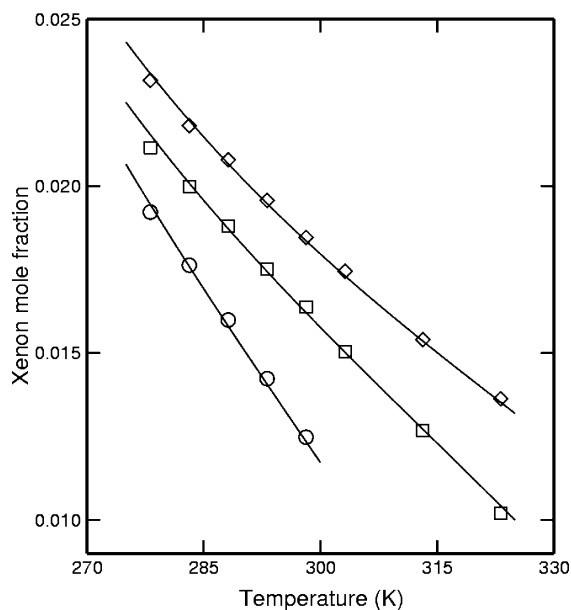


Figure 8. Solubility of xenon in linear perfluoroalkanes at 1 atm. Symbols represent experimental data³⁵ for *n*-perfluorohexane (circles), *n*-perfluoroheptane (squares), and *n*-perfluorooctane (diamonds) at 1 atm. Solid lines correspond to the predictions from the soft-SAFT EOS.

TABLE 2: Adjusted Binary Parameters for the Solubility of Xenon and Oxygen in Perfluoroalkanes, and AADs of the Calculations by the Soft-SAFT EOS with Respect to Experimental Data

	η	ξ	AAD (%)
Xe + <i>n</i> -C ₆ F ₁₄	0.797	0.816	2.4
Xe + <i>n</i> -C ₇ F ₁₆	0.877	0.816	2.0
Xe + <i>n</i> -C ₈ F ₁₈	0.888	0.816	0.7
O ₂ + <i>n</i> -C ₆ F ₁₄	1.116	0.320	4.5
O ₂ + <i>n</i> -C ₇ F ₁₆	1.381	0.829	3.4
O ₂ + <i>n</i> -C ₈ F ₁₈	1.599	1.044	4.0
O ₂ + <i>n</i> -C ₉ F ₂₀	1.921	1.200	2.0

predicted with the use of a single binary parameter. This parameter was adjusted using only the vapor–liquid equilibrium data near the azeotropic point of one mixture at a given temperature. This acts in favor of the transferability of the molecular parameters used.

It is known that xenon can be considered as the first member of the *n*-alkane series³⁶ in terms of phase equilibria properties. Because of this similarity, our model for xenon with perfluoroalkanes should also provide satisfactory results, as it occurred with *n*-alkane + *n*-perfluoroalkane mixtures. Additionally, differences in size have now a noticeable effect. We provide soft-SAFT predictions for the solubility of xenon in *n*-perfluorohexane, *n*-perfluoroheptane, and *n*-perfluorooctane at 1 atm, which are presented in Figure 8. The experimental data shown in this plot were calculated from the Ostwald coefficients reported in the literature³⁷ according to the procedure presented in ref 38. Binary interaction parameters were adjusted for each mixture, and they are listed in Table 2. Note that the energy binary parameter is set constant for all of the mixtures with xenon, as we did with the *n*-alkanes + *n*-perfluoroalkanes mixtures. Although the agreement is excellent (see also Table 2 for AADs), the predictive capability of the model and parameters cannot be tested for these mixtures at other conditions because, to our knowledge, there is no additional experimental solubility data available in the literature.

In principle, given that the soft-SAFT model without considering association has proved to provide reliable quantitative predictions for the xenon + *n*-perfluoroalkane and *n*-alkane +

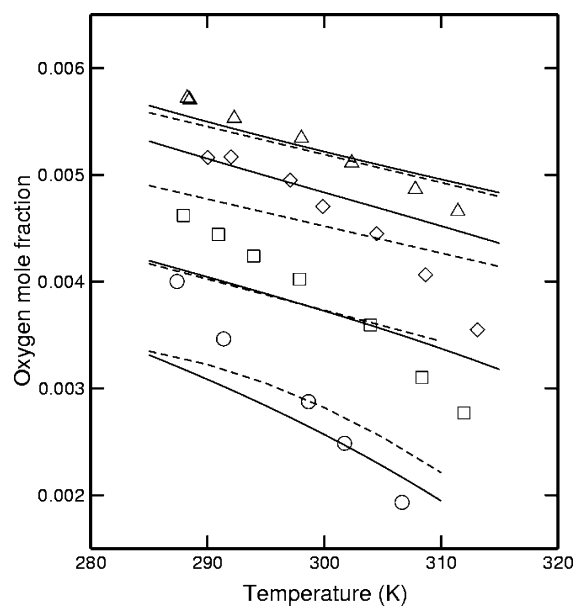


Figure 9. Solubility of oxygen in linear perfluoroalkanes at 1 atm. Symbols represent experimental data³⁸ for *n*-perfluorohexane (circles), *n*-perfluoroheptane (squares), *n*-perfluorooctane (diamonds), and *n*-perfluorononane (triangles). Lines correspond to the Peng–Robinson (dashed) and the soft-SAFT equations with the nonassociating model (solid).

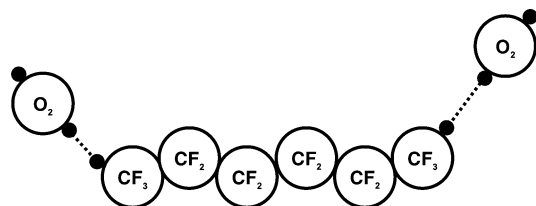


Figure 10. Two-dimensional sketch of the cross association model for the solubility of oxygen in *n*-perfluoroalkanes.

n-perfluoroalkane systems, one could expect a similar achievement for the solubility of oxygen in linear perfluoroalkanes. However, the comparison with our measurements, calculated from the Ostwald coefficients measured³⁸ and presented in Figure 9, shows that the soft-SAFT model without association inevitably predicts a much weaker dependence on temperature, regardless of the values of the binary interaction parameters. We also observed that the Peng–Robinson EOS does not provide a good trend either, as can be seen in Figure 9 as a dashed line (one binary parameter of the EOS was fitted to the experimental data³⁸). Because van der Waals interactions seemed to be correctly captured in the previous cases, one should think that additional interactions exist in this mixture, which are not considered by the model.

According to Mack and Oberhammer,³⁹ ab initio calculations of the interaction potentials for the complex CF₄–O₂ provide evidence that an interaction between the oxygen and the positive carbon nucleus in CF₄ occurs, forming a very strong complex. Admitting that the same interactions can be found between oxygen and higher order perfluoroalkanes, and that they may significantly affect equilibrium properties, the soft-SAFT model should account for this in some way. Therefore, we proposed to add the free energy of cross-association between oxygen and perfluoroalkane molecules to the total energy of the system. Consequently, both molecular oxygen and perfluoroalkanes were modeled as associating molecules with two association sites on each, as drawn in Figure 10. In the case of oxygen, sites represent the two lone pairs of electrons and, in the case of

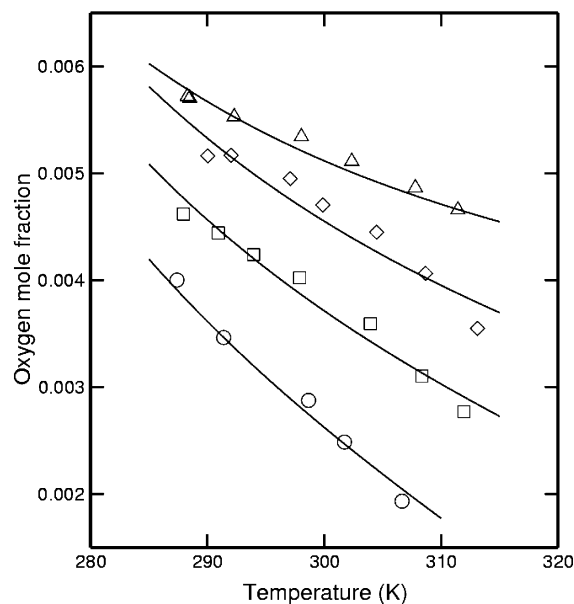


Figure 11. Solubility of oxygen in linear perfluoroalkanes at 1 atm. Symbols as in Figure 9. Lines correspond to the soft-SAFT EOS with the cross-associating model.

perfluoroalkanes, the two ends of the molecule where the carbon atoms are more exposed (less screened by the fluorine atoms). The magnitude of the site–site interaction between oxygen and perfluoroalkane molecules in the SAFT model depends on the two cross-association parameters, $\epsilon = 2000$ K and $k = 8000$ Å³, which were set constant for all mixtures. These values provide the proper solubility dependence with temperature, which was impossible to reproduce without the association model. Binary interaction parameters were then fitted for each mixture to experimental data, and they are listed in Table 2. Predictions of the soft-SAFT EOS with the associating model for the solubility of oxygen in perfluoroalkanes at 1 atm are shown in Figure 11 as solid lines, with the same experimental data shown in Figure 9. As can be observed, the soft-SAFT model that includes cross-association satisfactorily reproduces oxygen solubilities in perfluorocarbon chains, compared to experimental data, having an AAD below 5%. Furthermore, binary interaction parameters have a sound trend with respect to the carbon number of the perfluoroalkane chain, as seen in Figure 12. Because size and energy parameters for pure perfluoroalkanes increase and tend to a constant value as the chain length increases, the same behavior is expected for the binary parameters. However, note that, for the size binary parameter, the curvature is still not observed for this chain-length range.

Conclusions

A SAFT model and parameters for the solubility of xenon and oxygen in *n*-perfluoroalkanes are provided. It turns out that cross-association between oxygen and perfluoroalkanes has to be considered in order to capture the correct temperature dependence of the solubilities. As explained in the last section, this is supported by ab initio calculations reported in the literature, which suggest that strong interactions exist between molecular oxygen and the carbon atoms of the perfluorocarbon chains.

Predictions of the solubility of xenon and the VLE and LLE of *n*-alkane + *n*-perfluoroalkane mixtures with a nonassociating model are also given. Size and energy molecular parameters for the pure *n*-perfluoroalkanes were optimized by fitting to

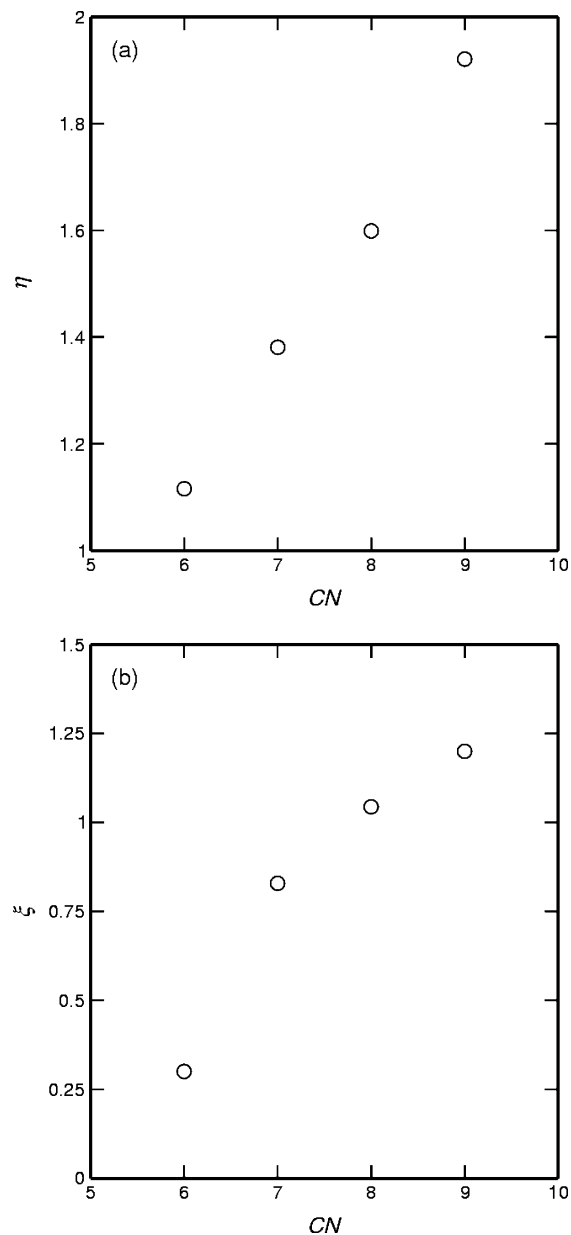


Figure 12. (a) Size and (b) energy binary parameters for the solubility of oxygen as a function of the carbon number of the *n*-perfluoroalkane.

experimental vapor pressures and saturated liquid densities. The chain-length parameter was taken from the values optimized in a previous work for the *n*-alkane series. Comparison of these optimized values to those from other models and the fact that they correlate as a function of the carbon number of the chain gives proof of their physical meaning and transferability.

Due to the high nonideality of the mixtures of this work, temperature independent binary interaction parameters need to be optimized. For *n*-alkane + *n*-perfluoroalkane mixtures of similar length, a unique optimized value of the binary energy parameter is used to describe VLE and LLE equilibrium properties in a broad range of temperatures with an AAD lower than 5% in most of the cases. Solubilities of xenon are predicted with a global AAD less than 2%.

For the solubility of oxygen, the AAD of predictions of the soft-SAFT model compared to experimental measurements is below 5%. Unique values for the two cross-association parameters were set and the optimized binary interaction parameters present an appropriate trend with respect to the perfluoroalkane chain length. We emphasize that a great advantage of using

SAFT is that it is possible to systematically improve the model to provide reliable and accurate predictions, provided that parameters remain meaningful, as shown in this work.

Acknowledgment. This work was financed by Fundação para a Ciência e Tecnologia, project PRAXIS XXI POCTI/1999/QUE/35435 and by Ministerio de Ciencia y Tecnología of Spain (integrated action HP2002-0089, and project PPQ2001-0671). A.M.A.D. is grateful to Fundação para a Ciência e Tecnologia (Ph. D. grant SFRH/BD/5390/2001). J.C.P. acknowledges a predoctoral grant from the Departament d'Universitats, Recerca i Societat de la Informació of the Generalitat de Catalunya, Spain.

References and Notes

- (1) Chechik, V.; Crooks, R. M. *J. Am. Chem. Soc.* **2000**, *122*, 1243.
- (2) Rao, N. S.; Baker, B. E. Textile Finishes and Fluorosurfactants. In *Organofluorine Chemistry: Principles and Commercial Applications*; Banks, R. E., Smart, B. E., Tatlow, J. C., Eds.; Plenum: New York, 1994; pp 321–336.
- (3) Raveendran, P.; Wallen, S. *J. Phys. Chem. B* **2003**, *107*, 1473.
- (4) Lowe, K. C. Properties and Biomedical Applications of Perfluorochemicals and Their Emulsions. In *Organofluorine Chemistry: Principles and Commercial Applications*; Banks, R. E., Smart, B. E., Tatlow, J. C., Eds.; Plenum: New York, 1994; p 555.
- (5) Miller, J. H., Jr.; Googe, J. M., Jr.; Hoskins, J. C. *Am. J. Ophthalmol.* **1997**, *123*, 705.
- (6) Wolber, J.; Rowland, I.; Leach, M.; Bifone, A. *Magn. Reson. Med.* **1999**, *41*, 442.
- (7) Cui, S. T.; Siepmann, J. I.; Cochran, H. D.; Cummings, P. T. *Fluid Phase Equilib.* **1998**, *146*, 51.
- (8) Watkins, E. K.; Jorgensen, W. L. *J. Phys. Chem. A* **2001**, *105*, 4118.
- (9) Bonifácio, R. P.; Filipe, E. J. M.; McCabe, C.; Costa Gomes, M. F.; Pádua, A. A. H. *Mol. Phys.* **2002**, *100*, 2547.
- (10) McCabe, C.; Galindo, A.; Gil-Villegas, A.; Jackson, G. *J. Phys. Chem. B* **1998**, *102*, 8060.
- (11) Blas, F. J.; Vega, L. F. *Mol. Phys.* **1997**, *92*, 135.
- (12) Blas, F. J.; Vega, L. F. *Ind. Eng. Chem. Res.* **1998**, *37*, 360.
- (13) Hesse, P.; Battino, R.; Scharlin, P.; Wilhelm, E. *J. Chem. Eng. Data* **1996**, *41*, 195.
- (14) Wilcock, R.; Battino, R.; Danforth, W.; Wilhelm, E. *J. Chem. Thermodyn.* **1978**, *10*, 817.
- (15) Makranczy J.; Megyery-Balog, K.; Ruzs, L.; Patyi, L. *Hung. J. Ind. Chem.* **1976**, *4*, 269.
- (16) Thomsen, E.; Gjaldback, J. *Acta Chem. Scand.* **1963**, *17*, 127.
- (17) Chapman, W.; Gubbins, K.; Jackson, G.; Radosz, M. *Fluid Phase Equilib.* **1989**, *52*, 31.
- (18) Huang, S.; Radosz, M. *Ind. Eng. Chem. Res.* **1990**, *29*, 2284.
- (19) Wertheim, M. S. *J. Stat. Phys.* **1984**, *35*, 19, 35; **1986** *42*, 459, 477.
- (20) Müller, E. A.; Gubbins, K. E. *Ind. Eng. Chem. Res.* **2001**, *40*, 2193.
- (21) Economou, I. *Ind. Eng. Chem. Res.* **2002**, *41*, 953.
- (22) Johnson, J.; Zollweg, J.; Gubbins, K. *Mol. Phys.* **1993**, *78*, 591.
- (23) Müller, E. A.; Gubbins, K. E. *Ind. Eng. Chem. Res.* **1995**, *34*, 3662.
- (24) Pàmies, J. C.; Vega, L. F. *Ind. Eng. Chem. Res.* **2001**, *40*, 2532.
- (25) Hariharan, A.; Harris, J. G. *J. Chem. Phys.* **101**, 4156.
- (26) NIST Chemistry Webbook, <http://webbook.nist.gov/chemistry>
- (27) Pàmies, J. C.; Vega, L. F. *Mol. Phys.* **2002**, *15*, 2519.
- (28) Kiselev, S. B.; Ely, J. F. *Fluid Phase Equilib.* **2000**, *174*, 93.
- (29) Caço A. I.; Dias, A. M. A.; Piñeiro, M.; Coutinho, J. A. P.; Marrucho, I. M. unpublished results.
- (30) Steele, W. V.; Chirico, R. D.; Knipmeyer, S. E.; Nguyen, A. J. *Chem. Eng. Data* **1997**, *42*, 1021.
- (31) Kreglewski, A. *Bull. Acad. Polonaise Sci.* **1962**, *10*, 11–12, p 876.
- (32) Florusse, L. J.; Pàmies, J. C.; Vega, L. F.; Peters, C. J.; Meijer, H. *AIChE J.* **2003** (in press).
- (33) Scott, R. L.; Van Konynenburg, P. H. *Discuss. Faraday Soc.* **1970**, *49*, 87.
- (34) Duce, C.; Tinè, M.; Lepori, L.; Matteoli, E. *Fluid Phase Equilib.* **2002**, *199*, 197.
- (35) Colina, C. M.; Galindo, A.; Blas, F. J.; Gubbins, K. E. *Proceedings of the 15th Symposium on Thermophysical properties*; Boulder, Colorado, 2003.
- (36) Filipe, E. J. M.; Dias, L. M. B.; Calado, J. C. G.; McCabe, C.; Jackson, G. *Phys. Chem. Chem. Phys.* **2002**, *4*, 1618.
- (37) Kennan, R.; Pollack, G. *J. Chem. Phys.* **1988**, *89*, 517.
- (38) Dias, A. M. A.; Freire, M. G.; Coutinho, J. A. P.; Marrucho, I. M. *Fluid Phase Equilib.* To be published.
- (39) Mack, H. G.; Oberhammer, H. *J. Chem. Phys.* **1987**, *87*, 2158.